

Document downloaded from:

<http://hdl.handle.net/10251/188032>

This paper must be cited as:

Traffano-Schiffo, MV.; Castro Giraldez, M.; Colom Palero, RJ.; Talens Oliag, P.; Fito, PJ. (2021). New methodology to analyze the dielectric properties in radiofrequency and microwave ranges in chicken meat during postmortem time. *Journal of Food Engineering*. 292:1-7. <https://doi.org/10.1016/j.jfoodeng.2020.110350>



The final publication is available at

<https://doi.org/10.1016/j.jfoodeng.2020.110350>

Copyright Elsevier

Additional Information

1 NEW METHODOLOGY TO ANALIZE THE DIELECTRIC PROPERTIES IN  
2 RADIOFREQUENCY AND MICROWAVES RANGE IN CHICKEN MEAT DURING  
3 POSTMORTEM TIME.

4 Maria Victoria Traffano-Schiffo a,\*, Marta Castro-Giraldez b, Ricardo J. Colom c, Pau Talens d, Pedro J.  
Fito b

5 a Instituto de Química Básica y Aplicada del Nordeste Argentino, IQUIBA-NEA, UNNE-CONICET, Avenida  
Libertad 5460, 3400, Corrientes, Argentina

6 b Instituto Universitario de Ingeniería de Alimentos para el Desarrollo, Universitat Politècnica de València,  
Camino de Vera s/n, 46022, Valencia, Spain

7 c Instituto de Instrumentación para Imagen Molecular, Universitat Politècnica de València, Camino de Vera s/  
n, 46022, Valencia, Spain

8 d Departamento de Tecnología de los Alimentos, Universitat Politècnica de València, Camino de Vera s/n,  
46022, Valencia, Spain

9

10 Correspondence should be addressed to Pedro J. Fito; [pedfisu@tal.upv.es](mailto:pedfisu@tal.upv.es); phone: +34963879832

11

12

13 **Abstract**

14 The biochemical and structural transformations that occur during the ageing of meat include proteolytic,  
15 electrolytic, oxidative and other processes, explain the quality and safety state of chicken meat. In this  
16 sense, the value of the dielectric properties at the relaxation frequency, in radiofrequency and microwave  
17 range have been used to monitor biochemical and structural transformations in some food processes, and  
18 can be a useful tool to predict the metabolic status of chicken meat. The aim of the work was to analyse the  
19 dielectric spectra during the post-mortem time in chicken meat, trying to understand and relate each  
20 dispersion phenomenon with the biochemical metabolism of meat ageing. 46 broiler breasts were analyzed  
21 at 5, 7, 9, 11, 13, 15, 17, 26, 50, 74, 98 and 146 h post-mortem. There were analyzed myofibrils proteins  
22 by DSC, pH, color, lactate by ion chromatography, dielectric properties in radiofrequency and microwaves  
23 and microstructure by Cryo-SEM. The proteolytic processes, main phenomenon in the ageing processes in  
24 meat, can be predicted directly through the evolution of the dielectric properties in  $\beta$ -dispersion, and finally,  
25 the results of this research work indicate that dielectric properties in  $\alpha$ ,  $\beta$  dispersions and the ionic  
26 conductivity could predict the post-mortem time in chicken meat.

27

28 *Keywords:* poultry meat, ageing, permittivity, radiofrequency, microwave.

## 30 1. INTRODUCTION

31 In the recent years, the consumption of poultry meat has had an accelerated growth and also an upward  
32 trend for the future is observed (Traffano-Schiffo et al. 2018a; Petracci et al. 2013). Particularly, the  
33 industry and consumers demand safety and high quality products. Due to this, meat ageing is one of the  
34 most influential factors that affects the final meat quality (Marino et al. 2013; Castro-Giráldez et al. 2011).  
35 Immediately after animal slaughter, complex structural and biochemical reactions are developed allowing  
36 the transformation of muscle to meat under controlled conditions (Ouali et al. 2006). These changes affect  
37 positively to the biological system, being the responsible for the tenderness, the juiciness and the flavour  
38 of the final product (Castro-Giráldez et al. 2011; Toldrá and Flores 1998). After animal slaughter, the lack  
39 of oxygen in the blood starts, thus, the aerobic glycolysis cannot continue and in order to maintain the ATP  
40 level needed to produce the vital metabolisms inside the muscle, the system follows an anaerobic pathway,  
41 obtaining lactic acid and adenosine monophosphate as final products, which mainly cause the drop of the  
42 pH (England et al. 2013) and the structural proteins degradation (Li et al. 2014). These metabolic  
43 transformations affect to the electric properties of the system.

44 The reduction of the pH of the muscle tissue causes the degradation of the myofibrillar structure and the  
45 increase of the liquid phase in sarcoplasmic and intercellular compartments. Intracellular and extracellular  
46 liquid phases are rich in ions with high mobility ( $\text{Ca}^{2+}$ ,  $\text{Cl}^-$ ,  $\text{K}^+$  and  $\text{Na}^+$ ) and also with  $\text{PO}_4^-$  (Pliquett et al.  
47 2003; Damez et al. 2008). Protein degradation is due to the action of some endogenous enzymes, such as  
48 calpains, cathepsin and calpastatin (Chéret et al. 2007; Herrera-Mendez et al. 2006), which are the main  
49 responsible of meat tenderness. It has recently been reported that the activity of  $\mu$ -calpain, m-calpain and  
50 calpastatin of chicken breasts at 48 h post-mortem decreases from  $0.55 \pm 0.04$  to  $0.28 \pm 0.05$ ;  $2.05 \pm 0.05$  to  
51  $1.99 \pm 0.01$  and  $1.52 \pm 0.01$  to  $1.19 \pm 0.03$  (Units/g), respectively (Biswas et al. 2016). On the other hand,  
52 during ageing, the original size of the proteins myosin, actin and troponin-T are reduced from 250 to 56  
53 kDa (Li et al. 2012); 43 to 32 kDa (Lametsch et al. 2002) and 70 kDa (Mudalal et al. 2014) to fragments of  
54 28, 30, 32 and 34 kDa (Huang et al. 2011), respectively.

55 In this context, sensors based in the analysis of the electromagnetic field (EMF) properties in range of  
56 radiofrequency (RF) and microwaves (MW) ranges could represent a useful and non-destructive tool to  
57 analyse the evolution of the ageing especially in chicken meat, where the degradative processes occur at  
58 higher speeds in comparison to other animal species.

59 The EMF is a flux of photons (Baker-Jarvid and Kim, 2012) and the interaction with matter can be modeled  
60 by Schrodinger's equation (Roychoudhuri et al., 2008) attending to the quantum theory. However, at  
61 macroscopic level, it is possible to apply the Maxwell's equations (Horie et al., 2000), where the physical  
62 property that describes the electric effect is the complex permittivity and for the magnetic effect is the  
63 complex permeability (Baker-Jarvid and Kim, 2012; Pozar, 1998). Both physical properties are vectorial,  
64 defining the sense of electric and magnetic field, being possible to minimize the effect of one or other  
65 depending on the geometry of the electrodes that generate the photons flux. Focusing on the permittivity,  
66 it can be explained as a complex number, where the real term or dielectric constant ( $\epsilon'$ ) is related to the  
67 electric energy storage by orientation and the imaginary term or dielectric loss factor ( $\epsilon''$ ) is related to the  
68 dissipation of the electric energy in others (Traffano-Schiffo et al. 2015; Talens et al. 2016). In RF and MW  
69 ranges, it is possible to distinguish different four effects along the electric spectra, three molecular  
70 orientation effects,  $\alpha$ ,  $\beta$ , and  $\gamma$  related with the storage and the dissipation, and one related with the molecular  
71 vibration ionic conductivity ( $\sigma$ ), related with the dissipation. The  $\alpha$ -dispersion, (Hz–kHz) is related with  
72 the charged molecules with high ionic strength, as electrolytes or organic acids (Kuang & Nelson 1998).  
73 The  $\beta$ -dispersion (kHz-MHz) is related with charged molecules, with high molecular weight and high  
74 quantity of charges (proteins, carbohydrates), and with the interfacial surfaces, with high surface tension  
75 charges (Traffano-Schiffo et al. 2017). The  $\gamma$ -dispersion (GHz), is related with the orientation and induction  
76 of the dipolar molecule such as water molecules (Castro-Giráldez et al. 2010a; Traffano-Schiffo et al.  
77 2018b).

78 Previously, some authors the useful of the dielectric properties as online control system by many authors  
79 to determine chicken meat quality (Ghatass et al. 2008; Castro-Giráldez et al. 2010b; Damez, & Clerjon  
80 2013; Traffano-Schiffo et al. 2018c), meat salting process (Castro-Giráldez et al. 2010c) and added water  
81 in meat (Kent, & Anderson 1996; Kent et al. 2002).

82 Some authors have published works on dielectric characterization of chicken in microwave range (Tanaka  
83 et al, 2000, Trabelsi, 2015; Zainal et al., 2016), or in radiofrequency (Mingjiang et al., 2011), some others  
84 in protein degradation processes in microwave (Bircanand et al., 2002), or in microwave cooking processes  
85 (Zhuang et al., 2007). Even in chicken ageing (Trabelsi, et al., 2016) where the authors worked with part  
86 of radiofrequency range and all microwave range. But few studies have analyzed the full spectrum of  
87 radiofrequency and microwaves by estimating the relaxation values of each dispersion, in order to  
88 understand complex biochemical processes and thus be able to monitor them accurately, as in chicken

89 qualities associated with premortem stress (Traffano et al. , 2018c), to myopathies (Traffano et al., 2017;  
90 Traffano 2018a). The use of models to obtain the relaxation values in the three dispersions has been used  
91 in human tissue (Miklavcic et al., 2006), in oncology processes in human breast(Lazebnik et al., 2007) or  
92 in tissue ageing in humans (Gabriel, 2005).

93 The aim of the work was to analyse the dielectric spectra during the post-mortem time in chicken meat, by  
94 using Traffano-Schiffo's model to obtain the the relaxation values of each dispersion, and try to understand  
95 and relate each dispersion phenomenon with the biochemical metabolism of meat ageing. Furthermore, the  
96 viability of using the dielectric spectroscopy as a useful tool to monitor the evolution of the meat ageing  
97 was analysed.

98

## 99 **2. MATERIALS AND METHODS**

100 For the experiments, 46 broiler breasts (*Pectoralis major*) from different birds, obtained from SADA Group  
101 slaughterhouse located in Rafelbunyol (Valencia, Spain), were used. After slaughter, male broilers of 42 d  
102 were bled out, plucked, tempered in a cooling tunnel at 4 °C for 3 h post-mortem and after that, the carcasses  
103 were collected at 4 h post-mortem and carried to the laboratory of the Institute of Food Engineering for  
104 Development (IuIAD) at the Polytechnic University of Valencia (UPV) using isothermal bags with ice  
105 blocks in order to maintain the samples at 2±1 °C. In the laboratory, the skin was removed and carcasses  
106 were deboned. The experiments were performed using chicken breasts (*Pectoralis major*) with 5 h post-  
107 mortem, maintaining them at 4 °C during the experimental procedure.

108 Considering previous experiments results, the selected times to follow the ageing process of chicken meat  
109 were: 5, 7, 9, 11, 13, 15, 17, 26, 50, 74, 98 and 146 h post-mortem.

110 The chicken breasts used to carried out this research were classified as normal following the classification  
111 of Zhang & Barbut (Zhang & Barbut, 2005).

112 At the indicated times, the following determinations were made. pH was measured as was explained in  
113 Traffano-Schiffo et al. (2018c). Protein phase transitions were obtained using a differential scanning  
114 calorimeter Mettler Toledo DSC 1 (Mettler Toledo, Barcelona, Spain) provided with the full range  
115 temperature sensor FRS5 as was explained by Traffano-Schiffo et al. (2018a). Mass fraction of proteins  
116 were obtained from the transition energies and the latent heat of denaturation of the pure proteins following  
117 the method of Traffano-Schiffo et al. (2018a).

118 The microstructure of chicken breasts was analysed by Cryo-SEM following the method of Traffano-  
119 Schiffo et al. (2018a). A Cryostage CT-1500C unit (Oxford Instruments, Witney, UK), coupled to a Jeol  
120 JSM-5410 scanning electron microscope (Jeol, Tokyo, Japan), was used.

121 Lactate quantification was determined by ion chromatography (Methrom Ion Analysis, Herisau,  
122 Switzerland), using a universal standard column (Metrosep Organic Acid 250 x 7.8 mm) and a precolumn  
123 along with an eluent composed of tartaric acid (4.0 mmol/L) and dipicolinic acid (0.75 mmol/L), equipped  
124 with electronic detectors. Samples were previously homogenized at 9000 rpm in an ULTRATURRAX T25  
125 for 10 min and centrifuged at 10000 rpm for 20 min (J.P. Selecta S.A., Medifriger-BL, Barcelona, Spain).  
126 Afterwards, 1 mL of supernatant was diluted with Milli<sup>®</sup>-Q water in a 50 mL Erlenmeyer flask. The clarified  
127 extract was filtered through a 0.45 µm Nylon Syringe Filter (Scharlab S.L., Barcelona, Spain); 15 mL was  
128 used to analyse the lactate content. Measurements were made in triplicate.

129 In addition, the pH and colour of samples were measured at 12 h post-mortem in order to classify the  
130 samples as normal following the classification of Zhang & Barbut (Zhang & Barbut, 2005). Colour of the  
131 samples was measured as was explained in Traffano-Schiffo et al. (2018c).

## 132 **2.1. Permittivity Measurements**

133 Permittivity of the samples was measured in the surface of the breasts (ventral side) in radiofrequency and  
134 microwave ranges. Measurements were non-destructive.

### 135 **2.1.1. Radiofrequency range**

136 The system used to obtain the impedance consists on a non-destructive sensor as was previously described  
137 by Traffano-Schiffo et al. (2018c). The estimation of  $\epsilon'$ ,  $\epsilon''$  from the impedance was calculated following  
138 the method Traffano-Schiffo et al. (2018c).

139 Finally, is possible to estimate the ionic conductivity using the loss factor, frequency and vacuum  
140 permittivity as follows:

$$141 \quad \sigma = \epsilon_0 \epsilon'' 2\pi f \quad (5)$$

142 Where  $\sigma$  is the conductivity expressed in  $\text{S}\cdot\text{m}^{-1}$ .

143

### 144 **2.1.2. Microwave range**

145 Permittivity in the microwave range was measured with an *Agilent* 85070E open-ended coaxial probe  
146 connected to an *Agilent* E8362B Vector Network Analyser (Agilent, Santa Clara, CA, USA). The system

147 was calibrated following the procedure of Traffano-Schiffo et al. (2018c). Permittivity measurements were  
148 measured in triplicate.

149

### 150 **2.1.3. Modelling of permittivity data**

151 The experimental data of the dielectric constant ( $\epsilon'$ ) were fitted by Traffano-Schiffo model (2017)  
152 (Equation 1), in order to obtain information the three dispersions that exist in RF and MW range:

$$\log \epsilon'(\omega) = \log \epsilon'_{\infty} + \sum_{n=1}^3 \frac{\Delta \log \epsilon'_n}{1 + e^{(\log \omega^2 - \log \tau_n^2) \cdot \alpha_n}} \quad (1)$$

153 Where n represents  $\alpha$ ,  $\beta$  or  $\gamma$  dispersion,  $\log \epsilon'$  represents the decimal logarithm of the dielectric constant,  
154  $\log \epsilon'_{\infty}$  the logarithm of the dielectric constant at high frequencies,  $\log \omega$  represents the decimal logarithm  
155 of the angular velocity (obtained from the frequency),  $\Delta \log \epsilon'_n$  ( $\Delta \log \epsilon'_n = \log \epsilon'_n - \log \epsilon'_{n-1}$ ) the amplitude  
156 of the n dispersion,  $\log \tau_n$  the logarithm of the angular velocity at relaxation time for each n dispersion, and  
157  $\alpha_n$  are the dispersion slopes.

158

159

### 160 **2.2. Statistical analysis**

161 The statistical analysis was carried out with the Statgraphics Centurion XVI Software (Statgraphics,  
162 Virginia, U.S.A.). One-Way ANOVA analyses were made in order to find statistically significant  
163 differences between the studied parameters. The logistic Traffano-Schiffo model (Traffano-Schiffo et al.,  
164 2017) was fitted by using nonlinear regression. Finally, the predictive algorithm was developed using the  
165 multiple regression tool.

166

## 167 **3. RESULTS AND DISCUSSION**

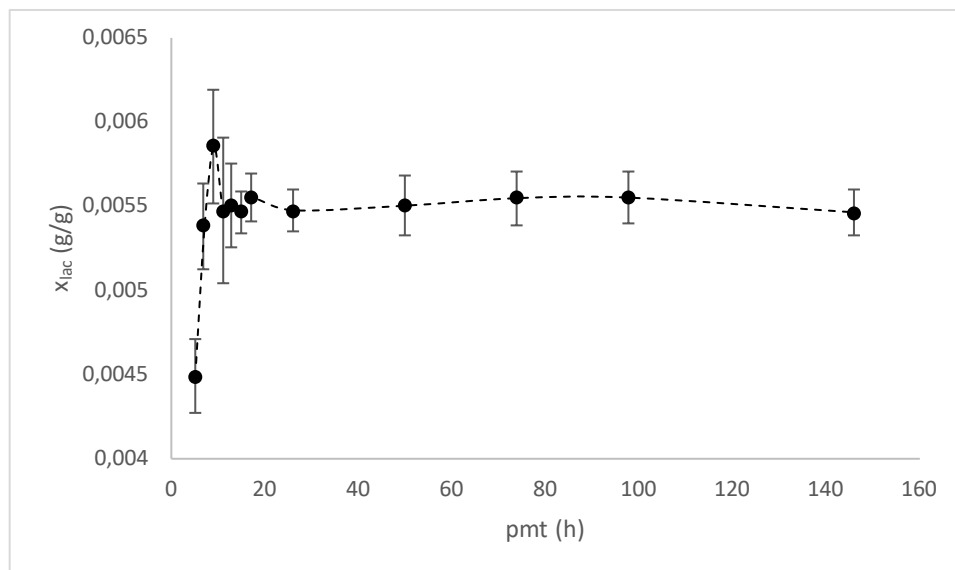
168 The biochemical transformations involved in the metabolisms of muscle transformation in meat implicate  
169 molecular changes that transform the electromagnetic equilibria in the animal tissue. By inducing a flux of  
170 photons through this tissue, it is possible to follow these metabolic transformations since they interfere in  
171 the trajectory and energy level of this flux of photons. To determine these transformations and their effect  
172 in the electromagnetic properties of photons in range of radiofrequency and microwaves, could allow the  
173 development of postmortem time prediction methodologies. In the metabolic processes that take place

174 during the postmortem of poultry meat, changes in the content and mobility of electrolytes, phosphates or  
175 lactate can produce changes both in the  $\alpha$ -dispersion and in the ionic conductivity (Traffano-Schiffo et al.,  
176 2018a). Changes in both myofibrillar and sarcoplasmic proteins will affect the  $\beta$ -dispersion (Traffano-  
177 Schiffo et al., 2018a, c), and overall structural changes will affect to the mobility of all chemical species  
178 and thus all three dispersions.

179 After animal slaughter, the blood flow stops, as well as the oxygen supply and, as a consequence, the aerobic  
180 glycolysis cannot continue. Muscle tries to maintain the homeostatic balance using glycogen as energy  
181 source in anaerobic conditions. Postmortem metabolism generates lactate, organic acids (Bates-Smith,  
182 1948; Farouk & Price, 1994; Moesgaard et al., 1995) and adenyphosphates are decomposed and inorganic  
183 phosphate is produced (Moesgaard et al., 1995). The liberation of electrolytes in the plasmalemma that  
184 cause a remarkable rise in ionic strength, is caused by the mechanisms of myofibrillar proteins proteolysis  
185 because of the inability of ATP dependent calcium, sodium, and potassium pumps to function (Huff et al.,  
186 2010). During the development of rigor mortis, ion concentration in liquid phase increases: sodium,  
187 magnesium, potassium, chloride, inorganic phosphate and lactate (Feidt & Brun-Bellut, 1999). These  
188 authors found a sodium, potassium and magnesium release of 82, 66 and 22% of total amount of the muscle,  
189 respectively. During the mechanisms of apoptosis the actin-myosin interaction is weakened by the depletion  
190 of ATP and the release of  $Mg^{2+}$  and  $Ca^{2+}$ , coupled with an increase in ionic strength (Li et al., 2012).  
191 Calcium ions concentration in chicken pectoral muscle was demonstrated to increase from 70  $\mu$ M after  
192 slaughter to 220  $\mu$ M after 18 hours of post-mortem, remaining constant around this quantity after 5 days of  
193 meat ageing (Ji & Takahashi, 2006).

194 Figure 1 shows the lactate evolution during post-mortem time; the lactate content increases rapidly during  
195 the first 7 hours post-mortem. After this moment, lactate content remains constant throughout the ageing  
196 of meat.





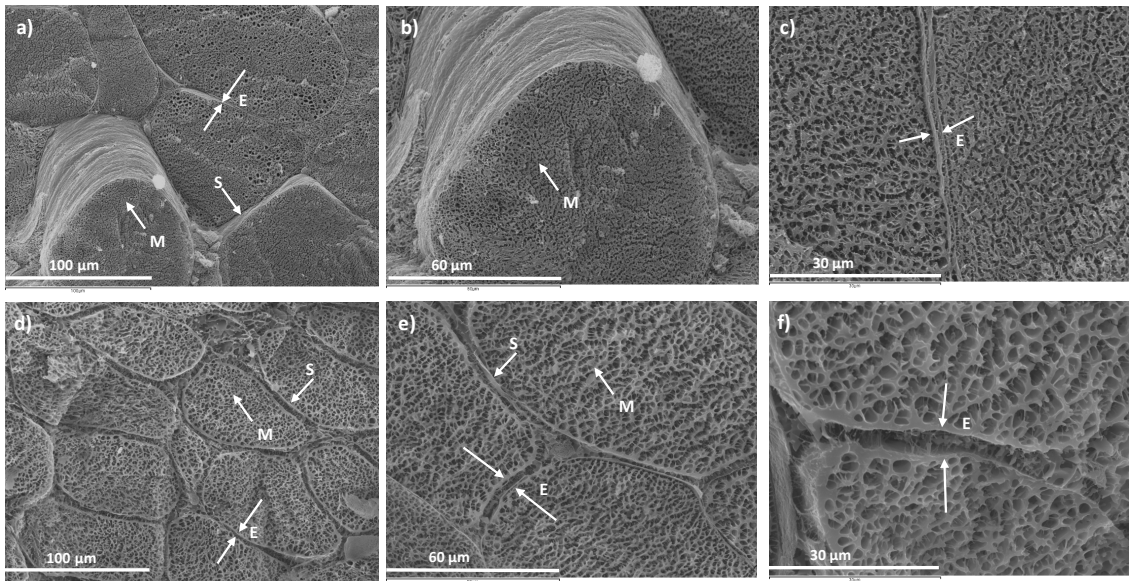
198 Figure 1. Lactate mass fraction evolution during post-mortem time.

199

200 The release of calcium is essential for the proteolytic processes associated with  $\mu$ -calpain and m-calpain,  
 201 responsible for the proteolysis of desmin and troponin (Goll et al., 1992), for protein oxidation in the  
 202 proteolysis of intermediate filaments such as titin or nebulin (Huff et al, 2010), and in general for the  
 203 apoptosis system that facilitates the proteolysis of the actin and myosin (Becila et al., 2010; Kemp & Parr,  
 204 2012).

205 In order to understand the structural changes during meat ageing, a low temperature scanning electron  
 206 microscopy was performed (Figure 2). Figure 2 shows a cross section of the muscle tissue of the chicken  
 207 breast, where the normal packaging of the myofibrils can be observed. Muscular fibres are involved by a  
 208 thin membrane or sarcolemma and in turn, these cells are interconnected by a connective tissue or  
 209 endomysium. Endomysium is the main responsible to maintain the myofibrils attached and to keep the  
 210 integrity and conformation of the muscle structure. Several differences between the micrographs at 5 and  
 211 12 h of pmt as a result of the ageing process can be appreciated. At 5 h of pmt, the myofibrillar space shows  
 212 a compact structure (Figure 2a, b and c); where the endomysium covers all the space between two adjacent  
 213 myofibrils, without leaving space for gaps between fibres. The average thickness of the endomysium is  
 214 around 3.5  $\mu\text{m}$ . At 12 h of pmt, the loss of muscle integrity, the endomysium inflammation and the  
 215 myofibrillar shrinkage can be appreciated (Figure 2 d, e and f). The average thickness of the endomysium  
 216 at this time is around 4.8  $\mu\text{m}$ , 37% higher comparing to 5 h of pmt. Also, big gaps can be appreciated.

217  
218



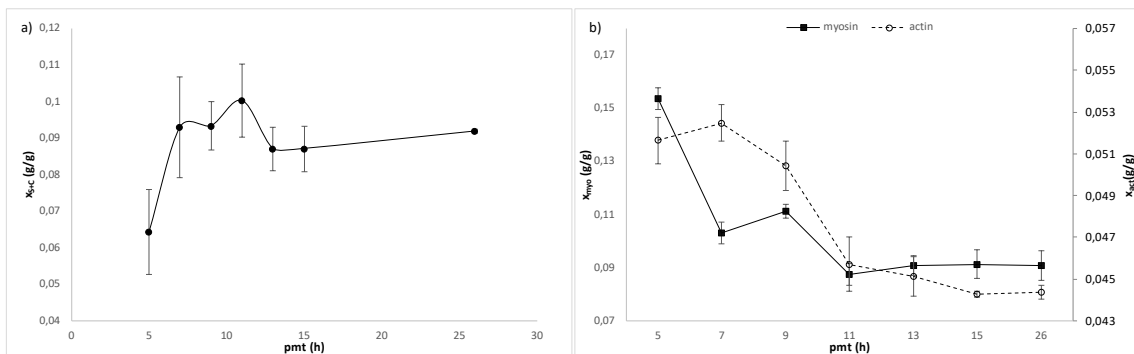
219

220 Figure 2. Micrographs of *Pectoralis major* chicken muscle. a, b and c, are samples of 5 h of pmt, d, e and f  
221 are samples of 12 h of pmt. a and d 500x, and b and e 1000x, c and f 5000x; where, E: endomysium; M:  
222 myofibrils and S: sarcolemma.

223

224 Post-mortem changes in protein degradation play a key role in the final meat quality (Hawkins et al. 2014).  
225 In order to analyse the thermal transitions of the meat proteins during the ageing evolution, DSC  
226 measurements were done. DSC curve of chicken meat shows five endothermal zones. The first peak around  
227 55 °C, is associated with myosin; the three central zones are related with collagen and sarcoplasmic proteins  
228 (between 63 to 76 °C) and the last one, at 80 °C with actin. Similar results were obtained by Fernández-  
229 Martín et al. (2000) and Ross (2006).

230

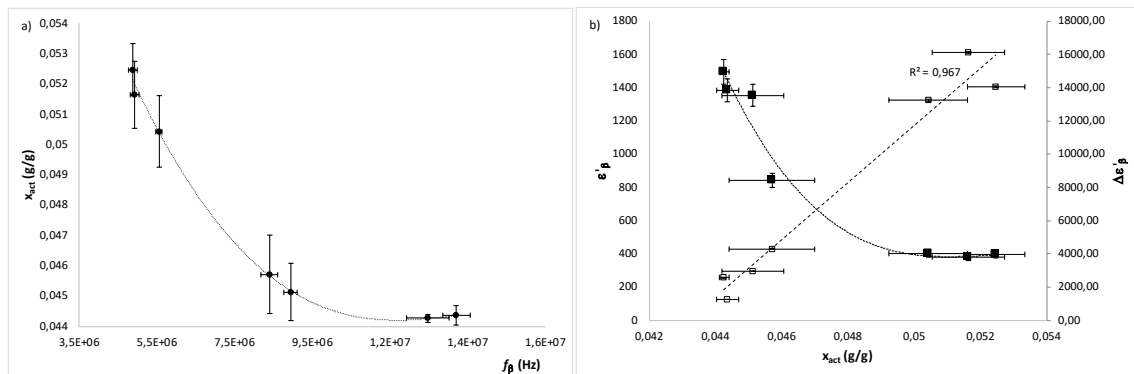


231 Figure 3. a) Evolution of sarcoplasmic and collagen (—●—) proteins mass fractions during the  
 232 postmortem time; b) Evolution of myosin (—■—) and actin (--○--) proteins mass fractions during the  
 233 postmortem time

234 Rigor mortis in chicken occurs in less than 6 hours after slaughter (Alvarado & Sams, 2000), in this process  
 235 the association of actin and myosin is produced irreversibly (Honikel et al., 1986). After this process,  
 236 ageing of meat is produced which involves the proteolysis and results in the fragmentation of myofibrils  
 237 and the lost of the integrity of muscle cells (Huff-Lonergan et al., 2010; Koohmaraie & Geesink, 2006).  
 238 The proteolytic process during the postmortem is complex since it is composed by different pathways. The  
 239 ( $\mu$ m) calpain, proteolytic enzyme, affects the thin filaments of the myofibrils, desmin and troponin-T,  
 240 weakening the strong actin-myosin interaction formed at pre-rigor facilitating its subsequent proteolysis  
 241 (Li et al., 2012). Other proteolytic mechanism is given by the caspase (Boatright & Salvesen, 2003), that  
 242 affect to the degradation of specific cytoskeletal proteins including actin (Green, 2011).

243 Oxidative stress has also been reported to increase both calpain and caspase-mediated degradation of  
 244 myofibrillar proteins, myosin heavy chain,  $\alpha$ -actinin, actin and troponin I in myofibrils, with increasing  
 245 levels of stress causing a stepwise escalation of proteolysis (Smuder et al., 2010). Figure 3a shows the  
 246 evolution of sarcoplasmic and collagen content with postmortem time. It is possible to observe an increase  
 247 in the content of these proteins during the 6 hours postmortem, after this time, the content remains stable  
 248 with postmortem time. Figure 3b shows the decrease in actin and miosin content with postmortem time, it  
 249 is possible to observe that the decrease is produced during the 11 hours of postmortem. Some authors  
 250 reported the degradation of both proteins during ageing (Hwang et al., 2005; Lametsch & Bendixen, 2001;  
 251 Lametsch et al., 2002; Lametsch et al., 2003)

252



253

254 Figure 4. a) Relationship between the actin mass fraction (g/g) and the relaxation frequency in  $\beta$ -dispersion  
255 during the pmt. b) Relationship between actin mass fraction (g/g) and dielectric constant in  $\beta$ -dispersion  
256 (■) and dielectric constant amplitude of  $\beta$ -dispersion (□) during the pmt.

257

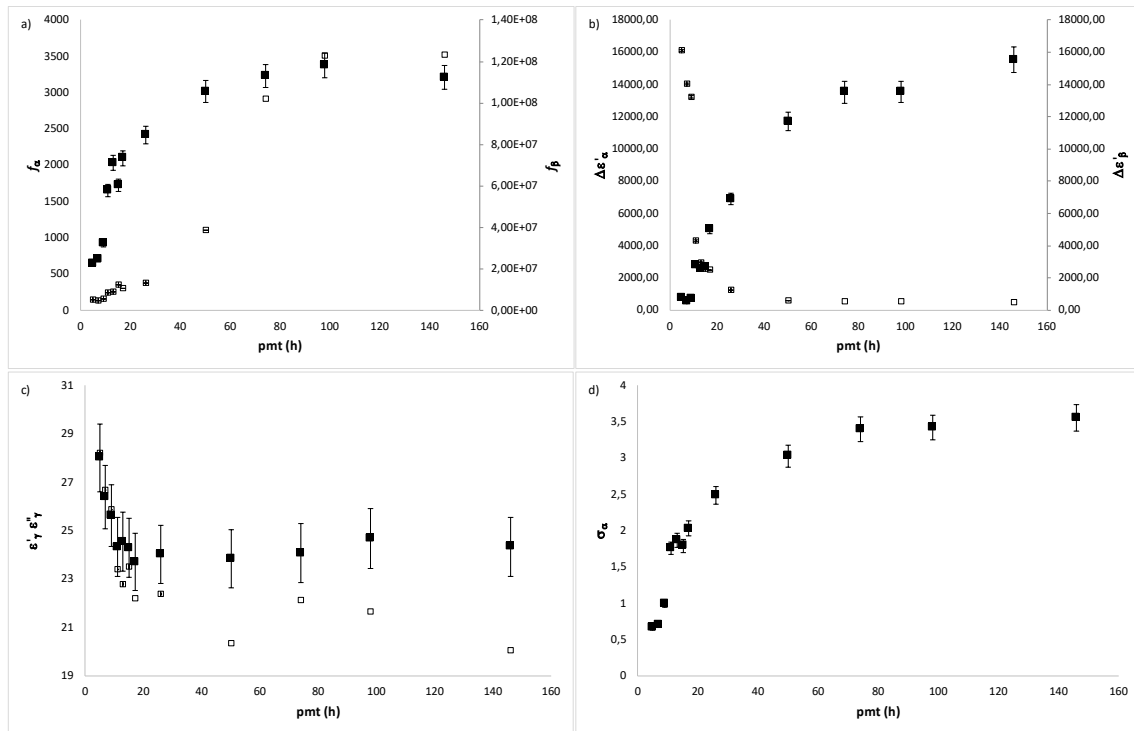
258 Figure 4a shows how the frequency of relaxation in the  $\beta$ -dispersion increases as the proportion of actin  
259 decreases, this occurs because the fragments of the actin complex that are proteolyzed are those of less  
260 molecular mass, leaving the proteins with higher molecular mass and generating a relaxation at a higher  
261 frequencies. However, these fragments are proteolyzed with a high number of active sites, they decrease  
262 the amplitude of  $\beta$ -dispersion, although they generate an increase in the absolute value of the dielectric  
263 constant in this dispersion, as shown in Figure 4b .

264 Therefore, as explained above, there are two phenomena that affect the circulation of photons through  
265 chicken tissue, the first is the release of electrolytes associated with the blockage of transport pumps, such  
266 as  $\text{Ca}^{2+}$ ,  $\text{Mg}^{2+}$ ,  $\text{Na}^+$ ,  $\text{K}^+$ , which causes an increase in the ionic strength of the medium. This phenomenon  
267 will affect both the  $\alpha$ -relaxation by the number of electrolytes to orientate and the conductivity of the  
268 medium, due to the increasing ionic strength. The second effect is the proteolysis of myofibrils, which  
269 generate changes in the properties associated with  $\beta$ -dispersion.

270 Figure 5 shows different dielectric properties in the dispersions  $\alpha$ ,  $\beta$  and  $\gamma$ , and the ionic conductivity with  
271 respect to the pmt. As Figure 5d shows, the ionic conductivity increases up to 80 h pmt due to the continued  
272 increase of the ionic strength associated with the release of electrolytes from the degradation of the transport  
273 pumps located in the protein tissue (Huff-Lonergan et al., 2010). This increase of the ionic strength also  
274 affects to the  $\alpha$ -dispersion as it can be observed in the amplitude of the dielectric constant (Figure 5b).  
275 These release of electrolytes is not homogeneous since some participate in the proteolysis of the ( $\mu$ /m)  
276 calpain as the  $\text{Ca}^{2+}$  and in the oxidative proteolysis as the  $\text{Mg}^{2+}$  and the  $\text{Ca}^{2+}$  (Li et al., 2012), for this reason  
277 the relaxation frequency of the  $\alpha$ -dispersion is changing with the pmt, as figure 5a shows.

278

279



280

281 Figure 5. a) Relationship between the relaxation frequency in  $\alpha$ -dispersion (■) and  $\beta$ -dispersion (□) during  
 282 the pmt. b) Relationship between the dielectric constant amplitude in  $\alpha$ -dispersion (■) and  $\beta$ -dispersion (□)  
 283 during the pmt. c) Relationship between the dielectric constant (■) and the loss factor (□) in  $\gamma$ -dispersion  
 284 during the pmt. d) Relationship between the ionic conductivity in  $\alpha$ -dispersion (■) during the pmt.

285

286 The proteolysis of the myofibrillar proteins causes a decrease in the amplitude of the dielectric constant in  
 287  $\beta$ -dispersion until 40 h pmt, as Figure 5b shows, following the post-rigor proteolytic metabolisms described  
 288 above. These proteolysis mechanisms also cause changes in the relaxation frequency of the  $\beta$ -dispersion  
 289 with respect to proteolysis (Figure 4a) and with respect to the pmt (Figure 5a).

290 Moreover, the proteolysis during the meat ageing causes a reduction in the water holding capacity (Bhat et  
 291 al., 2018) reducing the quantity and mobility of water molecules in the meat tissue. This phenomenon can  
 292 be observed in Figure 5c, in the reduction of the dielectric constant and the loss factor in  $\gamma$ -dispersion during  
 293 the first 20 h pmt.

294 Taking into account the effect of meat ageing in the  $\alpha$ ,  $\beta$  dispersions and the ionic conductivity, the  
 295 dielectric properties can be a useful tool to predict the pmt in chicken meat.

296 **4. CONCLUSIONS**

297 The proteolytic processes, main phenomenon in the ageing processes in meat, can be predicted directly  
298 through the evolution of the dielectric properties in  $\beta$ -dispersion.  
299 The results of this research work indicate that dielectric properties in  $\alpha$ ,  $\beta$  dispersions and the ionic  
300 conductivity could predict the post-mortem time in chicken meat.

## 301 5. ACKNOWLEDGEMENTS

302 The authors acknowledge the financial support from: the Spanish Ministerio de Economía, Industria y  
303 Competitividad, Programa Estatal de I+D+i orientada a los Retos de la Sociedad AGL2016-80643-R,  
304 Agencia Estatal de Investigación (AEI) and Fondo Europeo de Desarrollo Regional (FEDER).

305

## 306 REFERENCES

- 307 Biswas, A. K., Tandon, S., & Beura, C. K. (2016). Identification of different domains of calpain and  
308 calpastatin from chicken blood and their role in post-mortem aging of meat during holding at refrigeration  
309 temperatures. *Food Chemistry*, *200*, 315-321.
- 310 Castro-Giráldez, M., Fito, P. J., Chenoll, C., & Fito, P. (2010a). Development of a dielectric spectroscopy  
311 technique for determining key chemical components of apple maturity. *Journal of Agricultural and Food*  
312 *Chemistry*, *58*(6), 3761-3766.
- 313 Castro-Giráldez, M., Aristoy, M. C., Toldrá, F., & Fito, P. (2010b). Microwave dielectric spectroscopy for  
314 the determination of pork meat quality. *Food Research International*, *43*(10), 2369-2377.
- 315 Castro-Giráldez, M., Fito, P. J., & Fito, P. (2010c). Application of microwaves dielectric spectroscopy for  
316 controlling pork meat (*Longissimus dorsi*) salting process. *Journal of Food Engineering*, *97*(4), 484-490.
- 317 Castro-Giráldez, M., Toldrá, F., & Fito, P. (2011). Low frequency dielectric measurements to assess post-  
318 mortem ageing of pork meat. *LWT-Food Science and Technology*, *44*(6), 1465-1472.
- 319 Chéret, R., Delbarre-Ladrat, C., de Lamballerie-Anton, M., & Verrez-Bagnis, V. (2007). Calpain and  
320 cathepsin activities in post mortem fish and meat muscles. *Food Chemistry*, *101*(4), 1474-1479.
- 321 Damez, J. L., & Clerjon, S. (2013). Quantifying and predicting meat and meat products quality attributes  
322 using electromagnetic waves: An overview. *Meat Science*, *95*(4), 879-896.
- 323 Damez, J. L., Clerjon, S., Abouelkaram, S., & Lepetit, J. (2008). Beef meat electrical impedance  
324 spectroscopy and anisotropy sensing for non-invasive early assessment of meat ageing. *Journal of Food*  
325 *Engineering*, *85*(1), 116-122.

326 England, E. M., Scheffler, T. L., Kasten, S. C., Matarneh, S. K., & Gerrard, D. E. (2013). Exploring the  
327 unknowns involved in the transformation of muscle to meat. *Meat Science*, 95(4), 837-843.

328 Fernández-Martín, F., Fernández, P., Carballo, J., & Jiménez-Colmenero, F. (2000). DSC study on the  
329 influence of meat source, salt and fat levels, and processing parameters on batters pressurisation. *European*  
330 *Food Research and Technology*, 211(6), 387-392.

331 Ghatass, Z. F., Soliman, M. M., & Mohamed, M. M. (2008). Dielectric technique for quality control of beef  
332 meat in the range 10 kHz–1 MHz. *American-Eurasian Journal of Scientific Research*, 3(1), 62-69.

333 Hawkins, S. A., Bowker, B., Zhuang, H., Gamble, G., & Holser, R. (2014). Post-mortem chemical changes  
334 in poultry breast meat monitored with visible-near infrared spectroscopy. *Journal of Food Research*, 3(3),  
335 57.

336 Herrera-Mendez, C. H., Becila, S., Boudjellal, A., & Ouali, A. (2006). Meat ageing: Reconsideration of the  
337 current concept. *Trends in Food Science & Technology*, 17(8), 394-405.

338 Huang, M., Huang, F., Xue, M., Xu, X., & Zhou, G. (2011). The effect of active caspase-3 on degradation  
339 of chicken myofibrillar proteins and structure of myofibrils. *Food Chemistry*, 128(1), 22-27.

340 Kent, M., & Anderson, D. (1996). Dielectric studies of added water in poultry meat and scallops. *Journal*  
341 *of Food Engineering*, 28(3-4), 239-259.

342 Kent, M., Peymann, A., Gabriel, C., & Knight, A. (2002). Determination of added water in pork products  
343 using microwave dielectric spectroscopy. *Food Control*, 13(3), 143-149.

344 Kuang, W., & Nelson, S. O. (1998). Low-frequency dielectric properties of biological tissues: a review  
345 with some new insights. *Transactions of the ASAE-American Society of Agricultural Engineers*, 41(1), 173-  
346 184.

347 Lametsch, R., Roepstorff, P., & Bendixen, E. (2002). Identification of protein degradation during post-  
348 mortem storage of pig meat. *Journal of Agricultural and Food Chemistry*, 50(20), 5508-5512.

349 Li, P., Wang, T., Mao, Y., Zhang, Y., Niu, L., Liang, R., ... & Luo, X. (2014). Effect of ultimate pH on  
350 postmortem myofibrillar protein degradation and meat quality characteristics of Chinese yellow crossbreed  
351 cattle. *The Scientific World Journal*, 2014.

352 Li, S., Xu, X., & Zhou, G. (2012). The roles of the actin-myosin interaction and proteolysis in tenderization  
353 during the aging of chicken muscle. *Poultry Science*, 91(1), 150-160.

354 Marino, R., Albenzio, M., Della Malva, A., Santillo, A., Loizzo, P., & Sevi, A. (2013). Proteolytic pattern  
355 of myofibrillar protein and meat tenderness as affected by breed and aging time. *Meat Science*, *95*(2), 281-  
356 287.

357 Mudalal, S., Babini, E., Cavani, C., & Petracci, M. (2014). Quantity and functionality of protein fractions  
358 in chicken breast fillets affected by white striping. *Poultry Science*, *93*(8), 2108-2116.

359 Ouali, A., Herrera-Mendez, C. H., Coulis, G., Becila, S., Boudjellal, A., Aubry, L., & Sentandreu, M. A.  
360 (2006). Revisiting the conversion of muscle into meat and the underlying mechanisms. *Meat Science*, *74*(1),  
361 44-58.

362 Petracci, M., Sirri, F., Mazzoni, M., & Meluzzi, A. (2013). Comparison of breast muscle traits and meat  
363 quality characteristics in 2 commercial chicken hybrids. *Poultry Science*, *92*(9), 2438-2447.

364 Pliquett, U., Altmann, M., Pliquett, F., & Schöberlein, L. (2003). Py—a parameter for meat quality. *Meat*  
365 *Science*, *65*(4), 1429-1437.

366 Pozar, D.M. (1998). *Microwave Engineering*. (2nd ed., pp. 1-55). New York, USA: John Wiley & Sons  
367 Inc.

368 Ross, Y. H. (2006). Phase transitions and transformations in food systems. In D. R. Heldman, D. B. Lund  
369 (Eds.), *Handbook of Food Engineering* (pp. 287-352). FL: CRC Press.

370 Talens, C., Castro-Giraldez, M., & Fito, P. J. (2016). Study of the effect of microwave power coupled with  
371 hot air drying on orange peel by dielectric spectroscopy. *LWT-Food Science and Technology*, *66*, 622-628.

372 Toldrá, F., & Flores, M. (1998). The role of muscle proteases and lipases in flavor development during the  
373 processing of dry-cured ham. *Critical Reviews in Food Science*, *38*(4), 331-352.

374 Traffano-Schiffo, M. V., Castro-Giraldez, M., Colom, R. J., & Fito, P. J. (2015). Study of the application  
375 of dielectric spectroscopy to predict the water activity of meat during drying process. *Journal of Food*  
376 *Engineering*, *166*, 285-290.

377 Traffano-Schiffo, M. V., Castro-Giraldez, M., Colom, R. J., & Fito, P. J. (2017). Development of a  
378 spectrophotometric system to detect white striping physiopathy in whole chicken carcasses. *Sensors*, *17*(5),  
379 1024.

380 Traffano-Schiffo, M. V., Castro-Giraldez, M., Herrero, V., Colom, R. J., & Fito, P. J. (2018a). Development  
381 of a non-destructive detection system of Deep Pectoral Myopathy in poultry by dielectric  
382 spectroscopy. *Journal of Food Engineering*, *237*, 137-145.



383 Traffano-Schiffo, M. V., Castro-Giraldez, M., Colom, R. J., & Fito, P. J. (2018b). New Spectrophotometric  
384 System to Segregate Tissues in Mandarin Fruit. *Food and Bioprocess Technology*, 11(2), 399-406.

385 Traffano-Schiffo, M. V., Castro-Giraldez, M., Colom, R. J., & Fito, P. J. (2018c). Innovative photonic  
386 system in radiofrequency and microwave range to determine chicken meat quality. *Journal of Food*  
387 *Engineering*, 239, 1-7.

388 Zhang, L., & Barbut, S. (2005). Rheological characteristics of fresh and frozen PSE, normal and DFD  
389 chic

390 [50] Baker-Jarvis J.; Kim S. The Interaction of Radio-Frequency Fields With Dielectric Materials at  
391 Macroscopic to Mesoscopic Scales. *J Res Natl Inst Stand Technol*. 2012 117: 1–60. DOI:  
392 10.6028/jres.117.001

393 [51] Roychoudhuri C, Kracklauer AF, Creath K. The nature of light: What is a photon. CRC Press; NY:  
394 2008. DOI: 10.1201/9781420044256.

395 [52] Horie K, Ushiki H, Winnik FM. *Molecular Photonics*. Wiley, NY: 2000. DOI:  
396 10.1002/9783527613205.

397 Tanaka, F., Mallikarjunan, P., Kim, C., Hung, Y.C. (2000), Measurement of dielectric properties of  
398 chicken breast meat, *Journal of JSAM* 62(4): 109-119

399

400 Bircanand, C., Barringer, S.A. (2002) Determination of protein denaturation of muscle foods using the  
401 dielectric properties. *Jour. Food Sci.* (67) 202 – 205

402

403 Zhuang, H. Nelson, SO , Trabelsi, S. Savage EM (2007) Dielectric properties of uncooked chicken breast  
404 muscles from ten to one thousand eight hundred megahertz *Poultry science* Volume 86, Issue 11,  
405 November 2007, Pages 2433–2440

406

407 Zainal Z ,Abidin, Omar FN, Biak DRA (2016) Alternative for rapid detection and screening of pork,  
408 chicken, and beef using dielectric properties in the frequency of 0.5 to 50 GHz *International Journal of*  
409 *Food Properties* 19(5) Pages 1127-1138 |

410

411 Trabelsi S., Roelvink, J ., Russell RB (2016) Investigating the influence of aging on radiofrequency  
412 dielectric properties of chicken meat *Journal of Microwave Power and Electromagnetic Energy*  
413 48(4)

414

415 S Trabelsi – (2015) Variation of the dielectric properties of chicken meat with frequency and temperature.  
416 *Journal of Food Measurement and Characterization*, – Springer

417

418 Mingjiang Z., Richard P.Woola J. Xiaob Q. (2011) Investigating the Influence of Aging on  
419 Radiofrequency Dielectric Properties of Chicken Meat. *Applied Sci.&Manufacturing* 42(3) Pages 229-  
420 233

421 Lazebnik M.; Okoniewski M; Booske J.H.; Hagness S.C. (2007) Accurate Debye Models for Normal and  
422 Malignant Breast Tissue Dielectric Properties at Microwave Frequencies. *IEEE Microwave and Wireless*  
423 *Comp.* 17(12) 822-824

424

425 Gabriel (2005) Dielectric Properties of Biological Tissue:VariationWith Age. *Bioelectromagnetics*  
426 *Supplement 7:S12-S18*

427

428 Miklavčič D, Pavšelj N., Hart F.X. (2006) Electric Properties of Tissues. Wiley Encyclopedia of  
429 Biomedical Engineering, Copyright&2006 John Wiley & Sons, Inc  
430 **FIGURE LEGENDS**

431